International Journal of Sciences: Basic and Applied Research (IJSBAR)

ISSN 2307-4531
(Print & Online)

http://gssrr.org/index.php?journal=JournalOfBasicAndApplied

The Effects of Dual Acceptor (Na, N) Doping on Zn and O Sites in ZnO

M. A. Sayed[a*], M. Kamruzzaman[b]

[a,b]*Department of Physics, Begum Rokeya University, Rangpur, Rangpur-5400, Bangladesh*

Abstract

ZnO is an attracted semiconducting material because of the intriguing structural, electronic and optical properties as well as the properties can easily be tuned for applications. However, p-type doping is an essential research interest to overcome the hindering of the applications of n-type ZnO for next-generation advanced electronic and optoelectronic devices. In this article, we focus on the p-type acceptor mono (Na, N) and dual (Na-N) doping effects on the structural, electronic and optical properties of ZnO using first-principles calculations based on the density functional theory (DFT). Detailed DFT analysis reveals that the structure of ZnO distorted resulting in (Na, N) and (Na-N) doping, respectively. Band structure calculation highlights the confirmation of p-type ZnO for both types of doping introduced by acceptor impurity bands at the top of the valence band and pushing the Fermi level into the valence band. The band gap of ZnO is increased for Na and Na-N doping, while decreases for N doping. The widening of the band gap with Na and Na-N doping could be explained by Burstein Moss effect. In this study the band gap can be tuned in between 0.58 and 0.93 eV. Importantly, enhancement of the absorption and photoconductivity in the near band edge region attributed to (Na, N) and (Na-N) could be extended its applications in high-performance p-type based electronic and optoelectronic devices.

Keywords: DFT; p-type ZnO; dual acceptor; optoelectronic and electronic.

1. Introduction

Zinc oxide is an inorganic, non-toxic, odorless smiconductor with the formula of ZnO. ZnO possess three crystal structures among them Wurtzite is the most stable phase at the ambient conditions [1-2].

---

* Corresponding author.

It has a broad band gap (~3.37 eV) and huge exciton energy (~60 meV) [1] at room temperature (RT). Due to higher transparency and intriguing optoelectronics properties of ZnO, it can be employed in many special fields like as touch-plane displays [3], solar cells [4], laser diodes [5] chemical and gas sensors[6], light-emitting diodes [7], nano and information technology [8-12]. It manifests n-type conductivity due to the native donor defects [13], oxygen vacancies (V_o) and zinc interstitial (Zn_i) [14-15]. p-type ZnO is more difficult to form due to the effect of self-compensating and deeper acceptor level. To fabricate p-type ZnO, researchers have been chosen group-I and group V elements as acceptor dopants. Park and his colleagues [16] reported that group-I elements (Li, Na, K) make shallow acceptors, whereas group-V elements (N, P, As) behaves as deep acceptors. They also calculated the formation energy and concluded that Na substitution on Zn site (Na_{Zn}) is needed higher energy than N substitution on O site (N_O). Na is a suitable acceptor among them (Group-I) because it delivers high hole concentration ($3x10^{18}$ cm^{-3}) and possess shallow substitutional level (Na_{Zn}: 0.17 eV) [16]. To achieve p-type ZnO, many investigations have already done from the last few decades [17-19]. Different types of p-n devices were constructed using Na as a doping element [20]. The crystallite size increases, but the transmittance and the band gap decreases with the increase of Na doping in ZnO thin films prepared by using sol-gel technique [21-23]. Shan and his colleagues showed that the pulsed laser deposited Na doped ZnO thin film promoted the electrical, structural and optical properties [24]. The electronic structures was tuned theoretically by Wan and his colleagues [25]. Due to comparable ionic radius and electronic structure of N and O, N is another promising p-type dopant element from group-V. N-doped ZnO showed the instability at RT [26-29] and get promising results at higher doping concentration of N [30]. Dual doping is a successful procedure to tune electric and optical properties. There are few reports on the preparation of stable p-type ZnO using dual (N, P), (Li, N), (Cd, Li), (Ni, Co), (Li, Cu) and (N, Cu) etc. acceptor elements [31-37]. They obtained p-type ZnO due to launching shallow acceptor levels at the upper VB and also observed a distinct red shift at the absorption. It should be noted that there is no such report on dual (Na, N) doping effects on the structural, electronic and optical properties of ZnO. In addition, importantly dual acceptor doping is an efficient way to get p-type ZnO. Therefore, the reason is to choice Na and N dual acceptor to get p-type ZnO. Furthermore, a systematic theoretical study is still limited to a small number of p-type dopants, which may limits the better understanding of experimental observations. In the present study we use density functional theory (DFT) based on the generalized gradient approximation (GGA) which undereste the band gap calculations, caused by the lower exchange correlation between electrons. But this discrepancy doesn't affect the accuracy of the description of the p-type conductivity in doped ZnO. We believe that our study will be benefited for experimental observations and their potential applications. In this work, Na and N are substituted on Zn and O sites, respectively to investigate the effect of single acceptor dopant on ZnO. Dual acceptors (Na-N) are replaced on Zn and O sites in ZnO to explore the effects on the structural, electronic and optical properties of ZnO using density functional theory (DFT).

2. Methodology

This study is executed using DFT with the generalized gradient approximation (GGA) and Perdew, Burke and Ernzerhof (PBE) psedopotential [38], as implemented in the (Cambridge Serial Total Energy Package) CASTEP [39] code. The k-points *4×4×2* were used with cutoff energy of 400 eV. The experimental lattice parameters, $a=b=3.25$ *Å*, $c=5.21$ *Å*, $\alpha=\beta=90^0$, and $\gamma=120^0$ [40-42] were used in optimization process. The ZnO *(2×2×2)*

supercell consists of 32 atoms shown in Fig 1(a). The substitution is performed by introducing one Na atom on one Zn atom site is equivalent to *6.25%* in the supercell shown in Fig 1 (b). Similarly for *6.25%* N doping, one N is substituted on one O atom site is shown in Fig 1(c). For Na-N dual doping, one Na and one N atoms are replaced on one Zn and one O sites atoms, respectively, which is shown in Fig 1(d). The optimization is executed to get lattice parameters for pure, (Na, N) mono and dual (Na-N) doped ZnO of *2×2×2* supercell, these are included in table 1.

3. Results and Discussion

3.1 Crystal Structure

Table 1 shows the optimized lattice parameters for pure ZnO, mono (Na, N) doped ZnO and dual (Na-N) doped ZnO. The obtained lattice parameters are very close to the theoretical [37, 43-46, 50-51] and experimental [47-49, 50] reports. These optimized values reveal the perfection of computational method. It is also seen that the lattice constant *'a'* slightly decreases for mono (Na, N) doping while increases for dual (Na-N) doping. On the other hand, the value of *'c'* increases for all types of doping indicates that doped ZnO are oriented along c-axis. These results demonstrate that compressive stress acts along the a-axis and tensile stress acts along the c-axis.

Table 1: Calculated lattice parameters, volume, band gap, bond length and bond population of pure and doped ZnO.

Type of doping	**Method**	**Lattice Parameters**							
		***a* = b (Å)**	***c*(Å)**	***c*/*a***	**Volume *(Å³)***	**Band Gap *(eV)***	**Bond length**		**Bond population**
Pure ZnO	Theo.	3.298[a] 3.298[b] 3.258[c] 3.295[g]	5.290[a] 5.286[b] 5.220[c] 5.290[g]	1.60[a] 1.60[b] 1.60[c] 1.60[g]	49.82[a] 49.79[b] 47.98[c] 49.61[g]	0.73[a] 0.74[g]	Zn-O	1.9996	0.39
	Expt.	3.245[d] 3.250[e]	5.209[d] 5.210[e]	1.61[d] 1.61[e]	47.50[d] 47.60[e]				
Na-doped ZnO	Theo.	3.296[a]	5.372[a]	1.62[a]	50.53[a]	0.93[a]	Zn-O	1.9270	0.50
	Expt.	3.267[f] 3.204[i]	5.209[f] 5.138[i]	1.59[f] 1.60[i]	48.17[f] 45.70[i]		Na-O	2.1746	0.21
N-doped ZnO	Theo.	3.279[a] 3.286[h]	5.345[a] 5.310[h]	1.63[a] 1.61[h]	49.76[a] 49.51[h]	0.58[a] 0.69[i]	Zn-O	1.9691	0.45
	Expt.	3.256[d]	5.223[d]	1.60[d]	47.70[d]		Zn-N	1.9572	0.58
(Na-N) dual-doped ZnO	Theo.	3.307[a]	5.347[a]	1.61[a]	50.64[a]	0.90[a]	Zn-O	1.9302	0.50
							Na-O	2.1665	0.24
							Zn-N	1.9263	0.66
							Na-N	2.3489	0.01

[a]Present work, [g]Refs. [37], [b,c]Refs.[43-46], [e]Refs.[47], [d]Ref. [48], [f]Refs.[49], [i]Refs. [50], [h]Refs. [51].

The expansion and compression of the lattice parameters are attributed to different ionic radii of Zn *(0.74 Å)*, O *(1.40 Å)*, Na (*1.02 Å)* and N *(1.46 Å)* [52] are the main reason for this structural distortion. It is noticed from the Table 1 that the volume of Na and N doped ZnO varies compared with pure ZnO. The bond populations and length of undoped, mono (Na, N) and dual (Na-N) doped ZnO are also represented in Table 1. Due to the higher

Na-O bond length and lower bond population as compared to that of Zn-O of ZnO system indicates higher volume. For N-doped ZnO, the bond length of Zn-N and Zn-O is lower and bond population is larger than pure ZnO, which indicates decrease in volume. In case of Na-N dual-doped ZnO system, the increase of volume is clearly seen as compared to mono doping. This is happened because of higher bond length and lower bond populations of Na-O, Na-N as compared to Zn-O, is shown in Table 1.

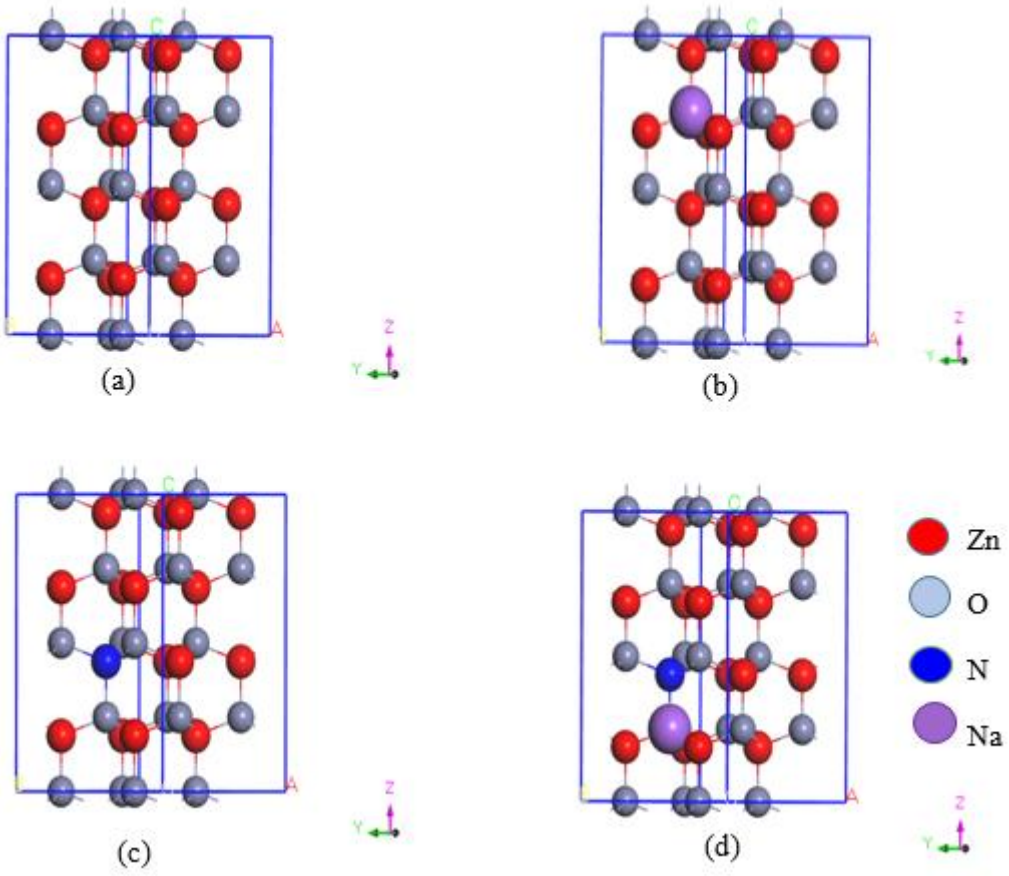

Figure 1: Crystal structure of (a) pure, (b) Na-doped, (c) N-doped and (d) Na-N dual doped ZnO.

3.2 Electronic Structure

3.2.1 Band Structure

Band structure analysis is very important in material science, which delivers many information of electronic, magnetic and optical properties of a matter. Figure 2 displayed the band structures of (a) pure, (b-c) mono (Na, N), and (d) dual (Na-N) doped ZnO. For all band structures, the valence band maximum (VBM) and conduction band minimum (CBM) lies along G-line, which reveals direct band gap. It is remarked that the calculated band gap of undoped ZnO is 0.73 eV (Fig.2a), which is in good agreement to the other theoretical results [37, 53-57]. While N is doped into ZnO (Fig.2c), the CB shifts towards the lower energy due to strong attraction between Zn-4s and N-2p states and introducing shallow acceptor level just top of the VB resulting in decrease the band gap. The calculated band gap of N-doped ZnO (Fig.2b) is 058 eV which is in good harmony with the other

theoretical results [50]. In case of dual (Na-N) doping ZnO (Fig.2d), again the CB moves toward the higher energy originated by the interaction among Zn-4s, N-2p and Na-2p, and acceptor impurity band is generated on the top of the VB, as a result the band gap of Na-N doped is increased. From figure 2, it is viewed that mono (Na, N), dual (Na-N) doped ZnO exhibits p-type semiconductor and the hole effective mass is higher for Na mono and dual (Na-N) doped than N-doped ZnO. More hole effective mass indicates more stable p-type semiconductor. So it can be concluded that Na and Na-N doped ZnO are more stable p-type semiconductor than N-doped ZnO.

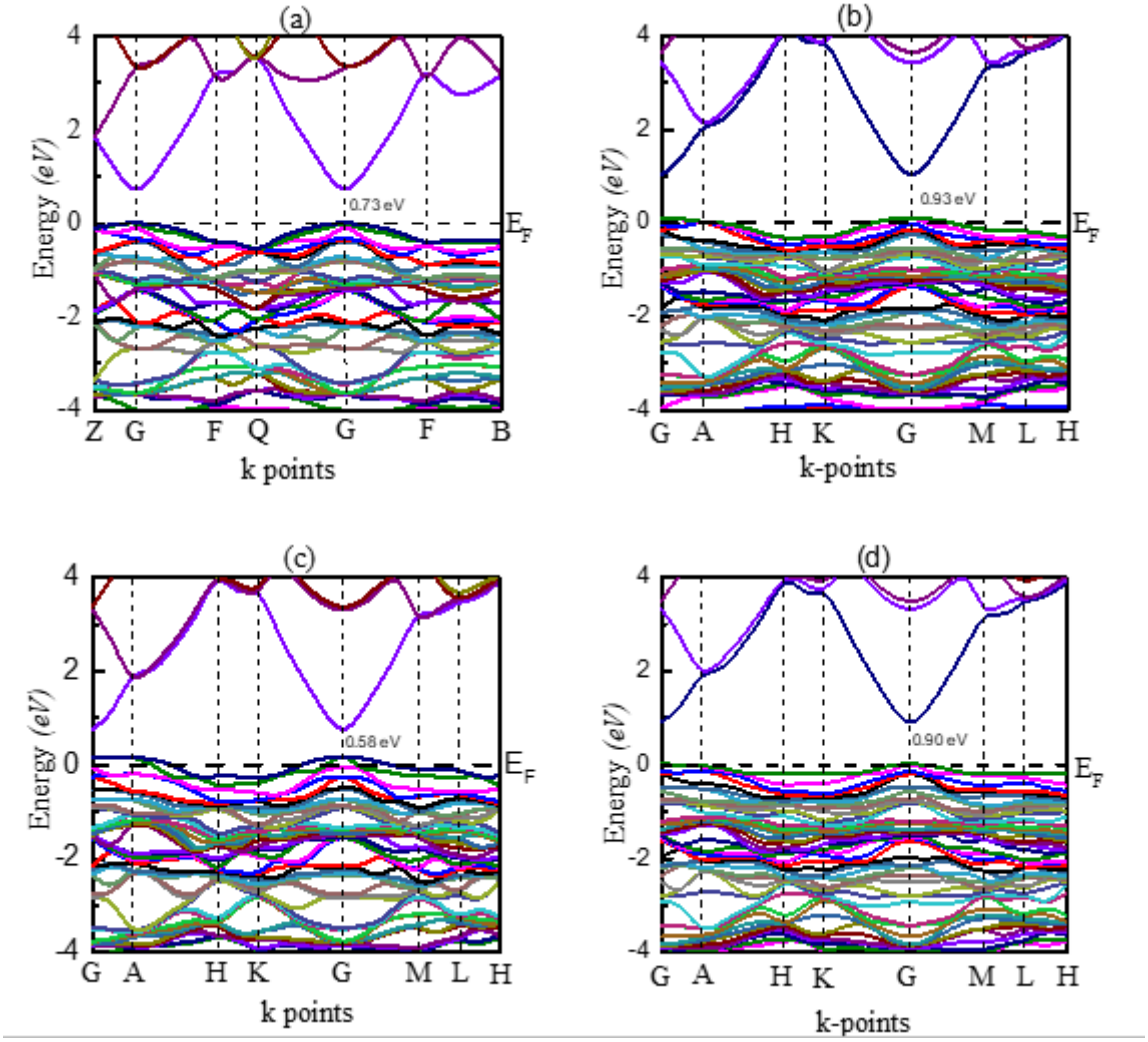

Figure 2: Band structures along high-symmetry k-points of (a) pure, (b) Na-doped, (c) N-doped and (d) Na-N dual doped ZnO.

But this theoretical band gap is so far from the experimental value (3.37 eV), which implies the inaccuracy in the value of band gap. This effect is occurred due to lower exchange correlation potential between electrons in GGA function. But the type of conductivity doesn't depends on this inaccuracy. From Fig.2b, it is seen that the band gap is increased for Na doping ZnO system resulting from shifting of the CB towards the higher energy attributed to the repulsion between Zn-4s and Na-2p states. It can also be seen that the impurity acceptor band is introduced above the valence band associated with the Fermi level shifts into valence band indicating p-type

nature of Na doped ZnO. While N is doped into ZnO (Fig.2c), the CB shifts towards the lower energy due to strong attraction between Zn-4s and N-2p states and introducing shallow acceptor level just top of the VB resulting in decrease the band gap. The calculated band gap of N-doped ZnO (Fig.2b) is 058 eV which is in good harmony with the other theoretical results [50]. In case of dual (Na-N) doping ZnO (Fig.2d), again the CB moves toward the higher energy originated by the interaction among Zn-4s, N-2p and Na-2p, and acceptor impurity band is generated on the top of the VB, as a result the band gap of Na-N doped is increased. From figure 2, it is viewed that mono (Na, N), dual (Na-N) doped ZnO exhibits p-type semiconductor and the hole effective mass is higher for Na mono and dual (Na-N) doped than N-doped ZnO. More hole effective mass indicates more stable p-type semiconductor. So it can be concluded that Na and Na-N doped ZnO are more stable p-type semiconductor than N-doped ZnO.

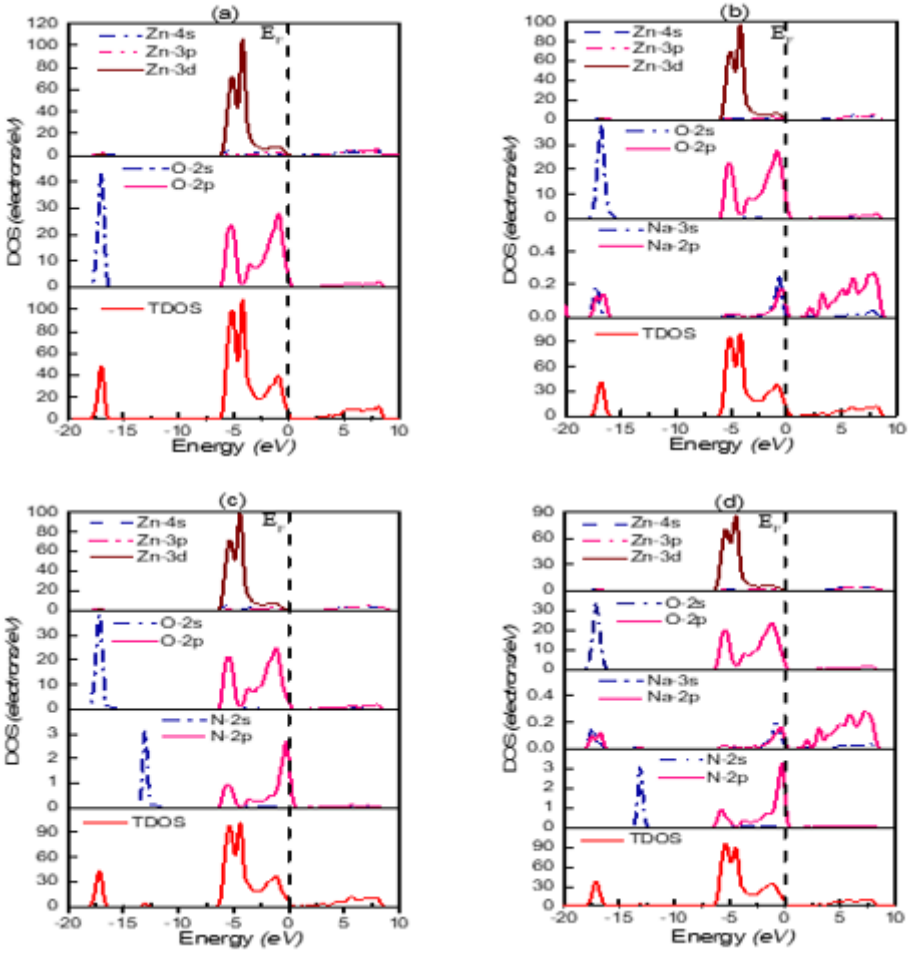

Figure 3: Total and partial density of states of (a) pure, (b) Na-doped, (c) N-doped and (d) Na-N dual doped ZnO.

3.2.2 Densities of state

The calculated total and partial densities of state (TDOS and PDOS) of pure, mono (Na, N) and dual (Na-N) doped ZnO is displayed in figure 3(a-d). To realize the effect of each atom in TDOS, the PDOS have been

calculated. The Fermi energy (E_F) is placed at zero energy. It is revealed from figure 3(a) that, the upper VB from 0 to -2.6 eV originates mainly from O-2p and the lower VB from -2.6 to 7.0 eV consisted by the hybridization coupling of Zn 3*d* and O 2*p* states. The core of the VB from -16.0 to 19.0 arisen from O-2s states with a small contribution of Zn-4s and Zn-3d states. The CB of pure ZnO is formed by the contribution of Zn-4s and O-2p states. In Na-doped ZnO, the upper valance band is consisted by the hybridization coupling among Na-3s, Na-2p, Zn-3d, and O-2p to generate acceptor level. Na-2p is also interacted with Zn-4s and O-2p and originated CB of Na-doped ZnO. The valence band is turned out by the hybridization coupling of Zn-4s, O-2p and N-2p levels and improved acceptor level of N-doped ZnO. Due to the strong interaction of Zn-4s and N-2p, the band gap reduced and the CB produced by the coupling of N-2p, O-2p and Zn-4s. The VB of dual (Na-N) doped ZnO is created by the interaction of following states of Zn-3d, O-2p, Na-2p and N-2p. The conduction band of dual doped ZnO is produced by the contribution of Na-2p and N-2p with the Zn-3p, O-2p states. The greater value of DOS at the upper VB related to mono (Na, N) and pure ZnO confirmed greater carrier concentrations to generate a p-type ZnO by dual (Na-N) doping. So, dual (Na-N) doping is more important to achieve stable p-type conductivity in ZnO.

3.3 Optical properties

3.3.1 Dielectric Constant

The usage of a material in optoelectronic devices depend on the optical properties of the material. Optical properties interpret the transition of the electron/hole between occupied and unoccupied states. There are two parts of dielectric constants: real $\varepsilon_1(\omega)$ and imaginary part $\varepsilon_2(\omega)$. The momentum matrix elements between the occupied and unoccupied wave functions are used to calculate the imaginary part $\varepsilon_2(\omega)$. Using $\varepsilon_2(\omega)$, the real part $\varepsilon_1(\omega)$ can be calculated by [58] equation. Refractive index n(ω), absorption coefficient α(ω), reflectivity R(ω), can be achieved by $\varepsilon_1(\omega)$ and $\varepsilon_2(\omega)$. Figure 4(a-b) represents the $\varepsilon_1(\omega)$ and $\varepsilon_2(\omega)$ spectra for different configuration of the ZnO system. For mono (Na, N) and dual (Na-N) doped ZnO, the static values of $\varepsilon_1(o)$ are 6, 10.3 and 15.15, respectively, which are larger than pure ZnO. The $\varepsilon_1(\omega)$ values decreases sharply with increases energy up to 1.20 eV. The $\varepsilon_1(\omega)$ is higher only for Na doped in the visible region. After visible range, they are possess approximately same value with pure ZnO. Figure 4(b) shows three important peaks located at 1.8, 6.4 and 9.4 eV, which represents the frequencies of intrinsic plasma of pure ZnO. The first peak (1.8 eV) originates from the electron transition between the states in the upper VB O-2p and lower CB Zn-4s states. The second peak (6.4 eV) may be arises from Zn-3d and O-2p transition in the VB. Another transition between the Zn-3d and O-2s states at around 9.10 eV. The height of the first peak increases and sifted to the lower energy for all configuration from pure ZnO. From density of states (Fig. 3(b-d)) it is observed that the peaks of O-2p and Zn-3d states are shifted toward lower energies due to doping effect.

3.3.2 Refractive index

There is a linear relation between $\varepsilon(\omega)$ and $n(\omega)$ by the relation of $n(\omega) = \sqrt{\varepsilon(\omega)}$, thus the shape of graph of $n(\omega)$ is identical with $\varepsilon(\omega)$. Figure 4(c-d) represents the graphs of real $n_r(\omega)$ and imaginary $n_i(\omega)$ refractive index for all configuration of ZnO. The $n_r(0)$ values 2.45, 3.20 and 3.6 for mono (Na, N) and dual (Na-N) doped ZnO are higher than the value (2.0) of pure ZnO. These values decrease sharply with increasing energy up to

1.2 eV.

At the visible region, the observed value of $n_r(\omega)$ lies in the range of 1.6-1.94. For large wavelength in the visible range $n_r(\omega)$ is larger for Na doped than others.After visible range, $n_r(\omega)$ decreases slowly and goes to under unity at around 10 eV for all configuration of ZnO. Electromagnetic wave travel faster than light velocity (c) after 10 eV energy, which indicates superluminal nature of material. The first peak of $n_i(\omega)$ is shifted toward the lower energy for mono (Na, N), dual (Na-N) doped ZnO. A similar effect is observed in case of $\varepsilon_2(\omega)$ which describes the optical transition of carriers from the VB and/or impurity to CB at the lower energy. The height of these first peaks represents the hole-electron generation in near the band edge energy. From figure 4(b) and (d), it is obvious that the height of the first peak is more intense for dual Na-N doped ZnO indicates the large amount of hole-electron pair's generation.

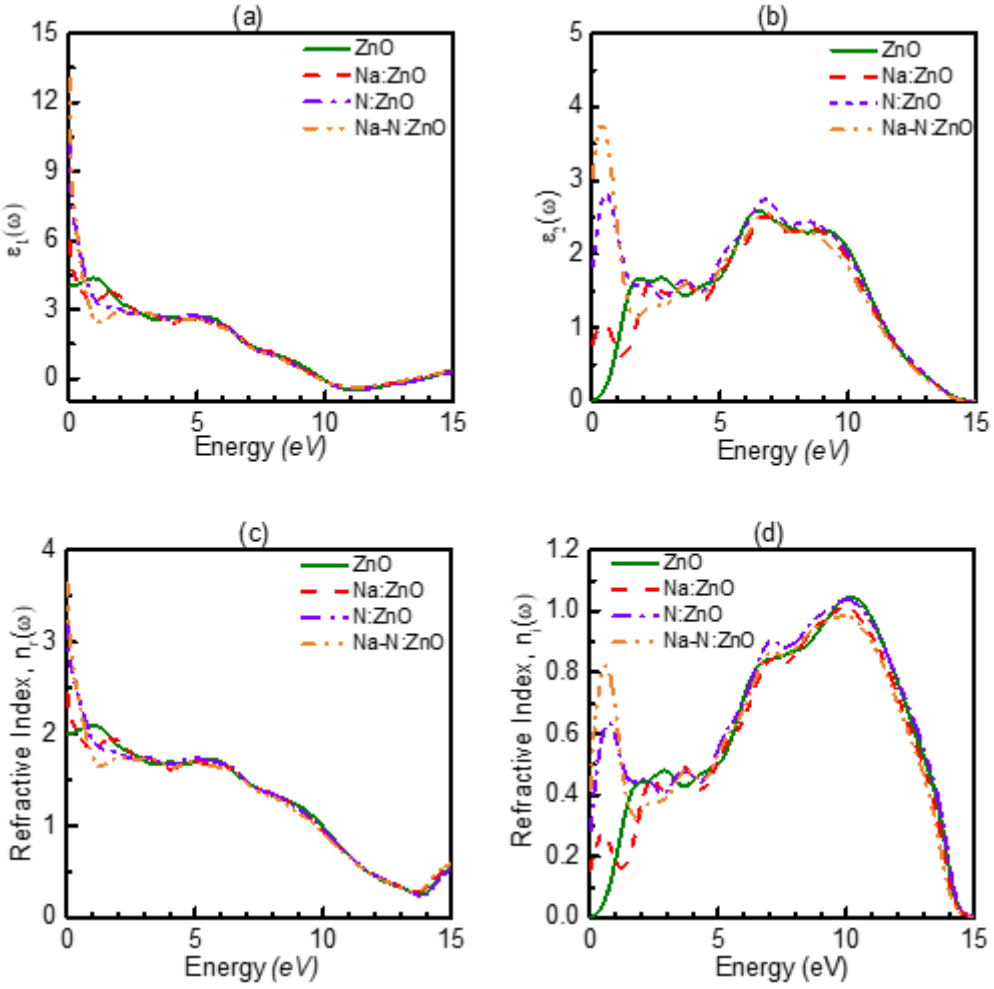

Figure 4: Calculated real and imaginary part of dielectric function and refractive indices of pure and doped ZnO.

3.3.3 Reflectivity

Reflectivity is an optical property of a material, which explains the returned energy from the material. It calculated by the relation $R(\omega) = \left|\frac{1-n(\omega)}{1+n(\omega)}\right|$, and shown in figure 5(a). The reflectivity at zero energy R(0) is 0.11 for pure ZnO and it increases up to 0.13 at 1.22 eV. The observed values of R(0) of mono (Na, N) doped and dual (Na-N) doped are 0.17, 0.28, and 0.33. It can be acclaimed that dual (Na-N) doped ZnO is better reflector than other for infrared radiation. Thus, the dual (Na-N) doped ZnO can be applicable into optoelectronic and electronic tools as a coating to protect from heat. Reflectivity is lower in the visible region than infrared and ultraviolet region. After visible region the shape of the reflectivity graph is opposite to the $n_r(\omega)$ graph. The value of R(ω) is zero above 15 eV (not shown here) for all configuration of ZnO, which implies that material becomes transparent above 15 eV.

3.3.4 Photoconductivity

The electrical conductivity can be increased by using photon energy. This property exists in semiconductor and enhance electrical conductivity. The photoconductivity can be calculated by the following formula $\sigma_r(\omega) = \omega\epsilon_0\varepsilon_2$ where ϵ_0 is the permittivity in free space and ε_2 is the real dielectric constant. The calculated optical conductivity shown in figure 5(b). The value of the initial peak near the band edge (0.58-0.93 eV) is greater for dual (Na-N) doped ZnO than other configurations. This greater value of the initial peak indicates the high concentration of electron-hole pairs generation. The prominent peaks (~9 eV) are decreased for doped ZnO with respect to pure ZnO and shifted towards the lower energy. This phenomena represents the probability of creating p-type semiconductor [21-23]. Finally, it can be noted from figure 5(b) that, dual (Na-N) doped ZnO is the most probable p-type semiconductor.

3.3.5 Absorption coefficient

By absorbing photon energy, the electron transfers from valence (occupied) to conduction (unoccupied) band. When the absorption coefficient α(ω) is higher, material absorbs more energy and increases the conductivity of the material. The α(ω) can be written by the following formula $\alpha(\omega) = \sqrt{2(\omega)}[\sqrt{\varepsilon_r^2 + \varepsilon_i^2} + \varepsilon_r(\omega)]^{\frac{1}{2}}$. Spectrum of α(ω) shown in figure 5(c). The first critical peak shifted into lower energy for all type doped configuration from pure ZnO peak, which indicates the direct band gap semiconductor. After these first peak, α(ω) increases with increase photon energy. From figure 5(c) it is observed that mono (Na, N) or dual doped ZnO can be used as a good absorber in the ultraviolet range 6 to 13 eV. The observed large prominent peak of pure ZnO is 17.6×10^4 at energy 10.7 eV. The magnitude of large peak for mono (Na, N) and dual (Na-N) doped ZnO is smaller and shifted into lower energy from pure ZnO, which represents the stability of p-type conductivity. It can be noted from figure 5(c) that, dual (Na-N) doped ZnO is the most probable p-type semiconductor. After 15 eV (not shown here), it is also seen that the material becomes as a transparent material. The band gap can be also calculated by using the Tauc's relation [59], $\alpha h\vartheta = A(h\vartheta - E_g)^n$, where A, hυ and E_g are the constant, photon energy and optical band gap. The tangent of $(\alpha h\vartheta)^2$ vs hυ graph represents the band gap. From figure 5(d), the observed band gap are to be 0.83, 0.98, 0.59 and 0.54 eV for pure, mono (Na, N) and dual doped ZnO, respectively which are close to the calculated band gap.

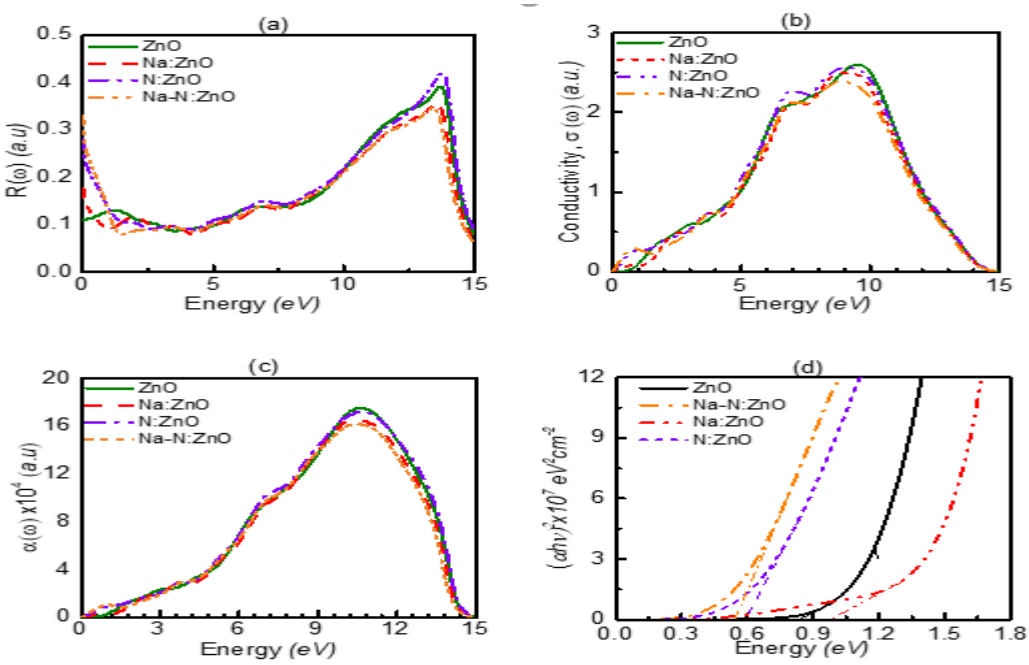

Figure 5: Calculated reflectivity, conductivity, absorptivity and Tauc plot of pure and doped ZnO.

4. Conclusions

A systematic first principles calculations have been performed of the effects of mono (Na, N) and dual (Na-N) doping on the structural, electronic and optical properties of ZnO. The optimized lattice parameters are in good agreement with the reports. The band structure calculation shows that all the structures are direct band gap semiconductor which are satisfactory values in comparison with reported results. The band gap is varied from 0.58 eV to 0.93 eV. The p-type nature is explicitly observed for all types of doping. The VB consists of Zn-3d, O-2p, Zn-3p; Na-3s, Na-2p, Zn-3d, O-2p, N-2p, Zn-3d, O-2p, Na-2p, N-2p and conduction band consists of Zn-3p, Zn-4s, O-2p; Zn-3p, O-2p; N-2p, O-2p, Zn-3p and Zn-3p, O-2p, Na-2p, N-2p of undoped, mono (Na, N) and dual (Na-N) doped ZnO, respectively. The absorption increases in the visible region for N and Na-N doped ZnO and also observed distinct red shift in the abosrption. The photoconductivity are significantly enhanced for all types of doping. The optical properties such as reflectivity, refractive index and dielectric constant have also been calculated. It can be concluded that dual (Na-N) doped ZnO is more stable p-type semiconductor than mono (Na, N) doped ZnO. Thus these obtained features of mono (Na, N) and Na-N dual doped ZnO would be suitable for modern optoelectronics devices.

Acknowledgments

Authors are thankful to Department of Physics Begum Rokeya University, Rangpur, Ragpur-5400, Bangladesh for providing computer facility.

5. Author Contributions

Both authors designed the study, interpreted the data and wrote the manuscript. They are equally contributed in

this work.

6. Declaration of Interest Statement

The authors declare no competing financial interests.

References

[1]. Ü. Özgür, Y. L. Alivov, C. Liu, A. Teke, M. A. Reshchikov, S. Doğan, V. Avrutin, S. J. Cho, H. Morkoç, "A comprehensive review of ZnO materials and devices," J. Appl. Phys., Vol. 98, pp. 041301, 2005.

[2]. M. Kamruzzaman, M. K .R. Khan, M. M. Rahman, M. Shahjahan M. R. Ahsan, M. A. S. Karal, "Electrical, Magnetic and Dielectric properties of $Zn_{1-x}Cd_xO$ system," International Journal of Modern Physics B, Vol. 25, pp. 3353-3360, 2011.

[3]. W. Dewald, V. Sittinger, B. Szyszka, F. Sauberlinch, B. Stannowski, D. Kohl, P. Ries, and M. Wuttig, "Advanced properties of Al-doped ZnO films with a seed layer approach for industrial thin film photovoltaic application," Thin Solid Films, Vol. 534, pp. 474, 2013.

[4]. Z. S. Wang, C. H. Huang, Y. Y. Huang, Y. J. Hou, P. H. Xie, B. W. Zhang, H. M. Cheng, "A Highly Efficient Solar Cell Made from a Dye-Modified ZnO-Covered TiO_2 Nanoporous Electrode," Chem. Mater., Vol. 13(2), pp. 678-682, 2001.

[5]. D. C. Look, B. Claflin, "P-type doping and devices based on ZnO," Phys. Status Solidi B, Vol. 241, pp. 624, 2014.

[6]. M. Hjiri, L. El Mir, S.G. Leonardi, A. Pistone, L. Mavilia, G. Neri, "Sens. Al-doped ZnO for highly sensitive CO gas sensors," Actuators B Chem., Vol. 196, pp. 413, 2014.

[7]. N. Saito, H. Haneda, T. Sekiguchi, N. Ohashi, I. Sakaguchi, K. Koumoto, "Low-Temperature Fabrication of Light-Emitting Zinc Oxide Micropatterns Using Self-Assembled Monolayers,". Adv. Mater., Vol. 14, pp. 418, 2012.

[8]. Y. L. Alivov, D. C. Look, B. M. Ataev, M. V. Chukichev, V. V. Mamedov, Y. A. Agafonov, A. N. Pustovit, "Fabrication of ZnO-Based Metal-insulator-Semiconductor Diodes by Ion Implantation," Solid State Electron, Vol. 48, pp. 2343-2346, 2014.

[9]. T. Makino, C. H. Chia, N. T. Tuan, Y. Segawa, M. Kawasaki, A. Ohtomo, K. Tamura, H. Koinuma , "Radiative and non radiative recombination processes in lattice-matched (Cd, Zn)O/(Mg, Zn)O multiquantum wells," Appl. Phys. Lett., Vol. 77, PP. 1632-1634, 2000.

[10]. D. C. Look, "Recent advances in ZnO materials and devices," Mater. Sci. Eng. B, Vol. 80, pp. 383-387, 2001.

[11]. F. Y. Zhang, J. Q. You, Z. Zeng, G. H. Zhong, "The effect of electronic orbital interactions on p-type doping tendency in ZnO series: First-principles calculations," Chin. Phys. B, Vol. 16, pp. 3815-3819, 2017.

[12]. F. C. Zhang, Z. Y. Zhang, W. H. Zhang, J. F. Yan, J. N. Yong, "First-principles study of the electronic and optical properties of ZnO nanowires," Chin. Phys. B, Vol. 18, pp. 2508-2513, 2009.

[13]. A. Janotti, G. Chris, Van de Walle, "New insights into the role of native point defects in ZnO," Journal

of Crystal Growth, Vol. 287, pp. 58–65, 2006.

[14]. S. B. Zhang, S. H. Wei, A. Zunger, "Intrinsic n-type versus p-type doping asymmetry and the defect physics of ZnO," A. Phys. Rev. B, Vol. 63, pp. 075205, 2001.

[15]. J. M. Bian, X. M. Li, X.D. Gao, W. D. Yu, L. D. Chen, "Deposition and electrical properties of N–In codoped p-type ZnO films by ultrasonic spray pyrolysis," Appl. Phys. Lett., Vol. 84 (4), pp. 541, 2004.

[16]. C. H. Park, S. B. Zhang, S. H. Wei, "Origin of p-type doping difficulty in ZnO: The impurity perspective," Physical Review B, Vol. 66, pp. 073202, 2002.

[17]. J. J. Lander, "Reactions of Lithium as a donor and an acceptor in ZnO," J. Phys. Chem. Solids, Vol. 15, pp. 324, 1960.

[18]. D. Zwingel, F. Gärtner, "Paramagnetic and Optical Properties of Na-Doped ZnO Single Crystals. Solid State Communications," Solid State Commun., Vol. 14, pp. 45, 2013.

[19]. D. Zwingel, "Trapping and recombination processes in the thermoluminescence of Li-doped ZnO single crystals," J. Lumin., Vol. 5, pp. 385, 1972.

[20]. R. Swapna, M. C. Santhosh, "Deposition of Na-N dual acceptor doped p-type ZnO thin films and fabrication of p-ZnO:(Na, N)/n-ZnO: Eu homojunction," Mater Sci. Eng. B-Adv, Vol. 178, pp. 1032-1039, 2013.

[21]. L.W. Wang, F. Wu, D.X. Tian, W.J. Li, L. Fang, C.Y. Kong, and M. Zhou, "Effects of Na content on structural and optical properties of Na-doped ZnO thin films prepared by sol–gel method," J. Alloys Compd., Vol. 623: pp. 367, 2015.

[22]. D. Akcan, A. Gungor, L. Arda, "Structural and optical properties of Na-doped ZnO films," Journal of Molecular Structure, Vol. 1161, pp. 299-305, 2018.

[23]. J. Lu, K. Huang, J. Zhu, X. Chen, X. Song, Z. Sun, "Preparation and characterization of Na-doped ZnO thin films by sol–gel method," Physica B, Vol. 405, pp. 3167–3171, 2010.

[24]. F. K. Shanl, G. X. Liu1, W. J. Lee, K. R. Bae, B. C. Shin, "Structural, Electrical, and Optical Properties of Na-Doped ZnO Thin Films Deposited by Pulsed Laser Deposition," Journal of Nanoscience and Nanotechnology, Vol. 8, pp. 5203–5207, 2008.

[25]. O. Wan, B. Shao, Z. Xiong, D. Li, G. Liu, "Theoretical Study of the Electronic Structures of Na-doped ZnO," Applied Mechanics and Materials, Vol. 665, pp.124-127, 2014.

[26]. S. Dhara, P.K. Giri, "Stable p-type conductivity and enhanced photoconductivity from nitrogen-doped annealed ZnO thin film," Thin Solid Films, Vol. 520, pp. 5000, 2012.

[27]. S. Nagar, S. Chakrabarti, "Realization of reliable p-type ZnO thin films by nitrogen implantation using plasma immersion ion implantation," Superlattices Microstruct., Vol. 75, pp. 9-16, 2014.

[28]. S. Golshahi, S.M. Rozati, A.M. Botelho do Rego, J. Wang, E. Elangovan, R. Martins, E. Fortunato, "Effect of substrate temperature on the properties of pyrolytically deposited nitrogen-doped zinc oxide thin films," Mater. Sci. Eng. B, Vol. 178, pp. 103, 2013.

[29]. T. K. Pathak, V. Kumar, H. C. Swart, L. P. Purohit, "Effect of doping concentration on the conductivity and optical properties of p-type ZnO thin films," Phys. B Condens. Matter, Vol. 480, pp. 31-35, 2016.

[30]. S. S. Shinde, C. H. Bhosale, K. Y. Rajpure, "Photocatalytic degradation of toluene using sprayed N-doped ZnO thin films in aqueous suspension," J. Photochem. Photobiol. B, Vol. 113, pp. 70-77, 2012.

[31]. T.H. Vlasenflin, M. Tanaka, "p-type conduction in ZnO dual-acceptor-doped with nitrogen and phosphorus," Solid State Communications, Vol. 142, pp. 292–294, 2007.

[32]. J. J. Yang, Q. Q. Fang, W. N. Wang, D. D. Wang, C. Wang, "Pulsed laser deposition of Li-N dual acceptor in p-ZnO:(Li, N) thin film and the p-ZnO: (Li, N)/n-ZnO homo-junctions on Si(100)," J. Appl. Phys., Vol. 115, pp. 124509, 2014.

[33]. J. G. Lu, Y. Z. Zhang, Z. Z. Ye, L. P. Zhu, L. Wang, B. H. Zhao, "Low-resistivity, stable p-type ZnO thin films realized using a Li–N dual-acceptor doping method," Appl. Phys. Lett., Vol. 88, pp. 222114, 2006.

[34]. M. Kamruzzaman, M. K. R. Khan, M. M. Rahman, M. A. S. Karal, M. Shahjahan, M. G. M. Chowdhury, "Synthesis and Characterization of $Zn_{1-x-y}Cd_xLi_yO_\delta$ Solid Solution," The Nucleus, Vol. 46 (1-2), pp. 37-42, (2009).

[35]. M. Kamruzzaman, J. A. Zapien, "Effect of Co and Ni on Au/$Zn_{1-x}M_xO$ Nanorods (M = Co and Ni) Schottky Photodiodes Performance," J. Nanosci. Nanotechnol., Vol. 17, pp. 5342–5351, 2017.

[36]. R. Afrose, M. Kamruzzaman, M. N. H. Liton, M. A. Helal, M. K. R. Khan, M. Rahman and T. K. Anam, "Synthesis and characterization of Zn100-xLixO and Zn100-x-yLixCuyO thin films for electronic and optoelectronic applications," International Journal of Modern Physics B, Vol. 33, pp. 1950257, 2019.

[37]. M. N. H. Liton, A. K. M. F. U. Islam, M. Kamruzzaman, M. K. R. Khan, M. A. Helal, M. M. Rahman, "Dual acceptor (N, Cu) doping effects on the electronic and optical properties of ZnO," Materials Chemistry and Physics, Vol. 242, pp. 122463, 2010.

[38]. J. P. Perdew, K. Burke, M. Ernzerhof, "Generalized Gradient Approximation Made Simple," Phys. Rev. Lett., Vol. 77, pp. 3865-3868, 1996.

[39]. M. D. Segall, P. Lindan, M. J. Probet, C. J. Pickard, P. J. Hasnip, S. J. Clark, M. C. Payne, "First-principles simulation: ideas, illustrations and the CASTEP code," J. Phys., Condens. Matter, Vol. 14, pp. 2717-2744, 2002.

[40]. R. D. Vispute, V. Talyansky, S. Choopun, P. P. Sharma, T. Venkatesan, M. He, X. Tang, J. B. Halpern, M. G. Spencer, Y. X Li, L. G. Salamanca-Riba, A. A. Iliadis, K. A. Jones, "Heteroepitaxy of ZnO on GaN and its implications for fabrication of hybrid optoelectronic devices," Applied Physics Letters, Vol. 73, pp. 348, 1998.

[41]. H. Y. Xia, C. Q. Xi, L. Z. Min, L. G. Fang, W. Y. Peng, W. Y. Ge, H. Y. Xia, C. Q. Xi, L. Z. Min, L. G. Fang, W. Y. Peng, W. Y. Ge, "First-principles calculation of microwave dielectric properties of Al-doping ZnO powders," Acta Physico-Chimic Sinica, Vol. 58, pp. 8002, 2009.

[42]. E. H. Kisi, M. M. Elcombe. "u parameters for the wurtzite structure of ZnS and ZnO using powder neutron diffraction," Acta Cryst. C, Vol. 45, pp. 1867-1870, 1989.

[43]. Y. G. Rui, F. G. Han, Z. S. Wen, M. J. Hong, C. Jun, Z. Yong, L. S. Ti, S. S. Chen, Z. Tao, "First-principles study of p-type ZnO by Te-N codoping," Acta Phys. Sin., Vol. 61(17), pp. 176105-7, 2012.

[44]. Z. C. Ying, W. Jing, B. Y. Lei, "First-principles investigation of N Ag co-doping effect on electronic properties in p-type ZnO," Chin. Phys. B, Vol. 19(4), pp. 047101-7, 2010.

[45]. S. F. Decremp, F. Datchi, A. M. Saitta, A. Polian, S. Pascarelli, A. DiCicco, J. P. Itie, F. Baudelet, "Local structure of condensed zinc oxide," Phys. Rev. B, Vol. 68, pp. 104101-10, 2013.

[46]. J. E. Jaffe, J. A. Snydern, Z. Lin, A. C. Hess, "LDA and GGA calculations for high-pressure phase transitions in ZnO and MgO," Phys. Rev. B, Vol. 62, pp. 1660-1665, 2010.

[47]. R. Baghdad, B. Kharroubi, A. Abdiche, M. Bousmaha, M. A. Bezzerrouk, A. Zeinert, M. E. Marssi, K. Zellama, "Mn doped ZnO nanostructured thin films prepared by ultrasonic spray pyrolysis method," Superlatt. Microstruct., Vol. 52, pp. 711-721, 2012.

[48]. M. N. H. Liton, K. K. R. Khan, M. M. Rahman, M. M. Islam, "Effect of N and Cu Doping on Structure, Surface Morphology and Photoluminescence Properties of ZnO Thin Films," J. Sci. Res., Vol. 7(1), pp. 23-34, 2015.

[49]. M. A. Basyooni, M. Shaban, A. M. El Sayed, "Enhanced Gas Sensing Properties of Spin-coated Na-doped ZnO Nanostructured Films," Scientific Reports, Vol. 7, pp. 41716, 2016.

[50]. S. M. Karadeniz, H. K. B. Çiplak, A. E. Ekinci, "Synthesis and Characterization of Na Doped ZnO Rods Grown by Simple Chemical Method," Materials Science (MEDŽIAGOTYRA), Vol. 26(4), pp. 387-391, 2020.

[51]. M. N. H. Liton, M. K. R. Khan, M. M. Rahman, "Effect of N and Al-N dual doping on optical, photoluminescence and transport properties of ZnO films," Mater. Res. Express, Vol. 2, pp. 065903–065909, 2015.

[52]. R. D. Shannon, "Revised effective ionic radii and systematic studies of interatomic distances in halides and chalcogenides," Acta Crystallographica, Vol. 32(5), pp. 751–767, 1976.

[53]. X. Si, Y. Liu, W. Lei, J. Xu, W. Du, L. Jia, T. Zhou, L. Zheng, "First-principles investigation on the optoelectronic performance of Mg doped and Mg–Al co-doped ZnO," Materials and Design, Vol. 93, pp. 128–132, 2016.

[54]. Z. Ming Z, Z. C. Hui, S. Jiang, "First-principles calculation of electronic structure of $Mg_xZn_{1-x}O$ codoped with aluminium and nitrogen," Chin. Phys. B, Vol. 20, pp. 017101, 2011.

[55]. P. Yang, Y. F. Zhao, H. Y. Yang, "Investigation on optoelectronic performances of Al, N codoped ZnO: First-principles method," Ceram. Int., Vol. 41, pp. 2446–2452, 2015.

[56]. R. Chowdhury, P. Rees, S. Adhikari, F. Scarpa, S. P. Wilks, "Electronic structures of silicon doped ZnO," Physica B, Vol. 405, PP. 1980-1985, 2010.

[57]. M. Bousmaha, M. A. Bezzerrouk, R. Baghdad, K. Chebbah, B. Kharroubi, B. Bouhafs, "Realization of p-Type Conductivity in ZnO via Potassium Doping," Acta Physica Polonica A, Vol. 129, pp. 1155-1158, 2016.

[58]. R. De L Kronig, "On the Theory of Dispersion of X-Rays," Journal of the Optical Society of America, Vol. 12 (6), pp. 547-557, 1926.

[59]. S. T. Tan, B. J. Chen, X. W. Sun, W. J. Fan, "Blueshift of optical band gap in ZnO thin films grown by metal-organic chemical-vapour deposition," J. Appl. Phys., Vol. 98, pp. 013505-5, 2005.